Polymer 51 (2010) 3315–3319

Contents lists available at ScienceDirect

Polymer

journal homepage: www.elsevier.com/locate/polymer

Self-assembly of linear ABC coil-coil-rod triblock copolymers

Yingdong Xia [a], Jizhong Chen [a,*], Zhaoyan Sun [a], Tongfei Shi [a], Lijia An [a,**], Yuxi Jia [b]

[a] State Key Laboratory of Polymer Physics and Chemistry, Changchun Institute of Applied Chemistry, Chinese Academy of Sciences, 5625 Renmin street, Changchun 130022, China
[b] School of Materials Science and Engineering, Shandong University, Jinan 250061, China

ARTICLE INFO

Article history:
Received 26 March 2010
Received in revised form
26 April 2010
Accepted 28 April 2010
Available online 11 May 2010

Keywords:
Coil-rod
Self-assembly
Self-consistent-field lattice

ABSTRACT

Self-assembly of linear ABC coil-coil-rod triblock copolymer melt is studied by applying self-consistent-field lattice techniques in three-dimensional (3D) space. In contrast to rod–coil diblock copolymers, our results reveal the effect of the broad parameter space on the self-assembly of the linear ABC coil-coil-rod triblock copolymers. Seven stable structures are found stable, including "two-color" lamella, "three-color" lamella, "two-color"-perforated lamella, "three-color"-perforated lamella, core-shell hexagonal lattice phase, strip, and micelle. When the two coil blocks have equal lengths ($f_A = f_B$), the lamellar structure dominates the majority of the phase diagram. The effects of the two coil blocks on the self-assembly are explored by tuning the relative length of the A and B coil blocks in terms of keeping the length of the block C (rod). Moreover, by switching the position of the blocks B and C, the influence of the block sequencing on the self-assembly is studied.

1. Introduction

Rod–coil block copolymers have received much attention due to their abilities to self-assemble 10–100 nm length scale structures in the field of novel functional and biomimetic materials.[1,2] Especially, the rod–coil block copolymers containing conjugated rod building blocks offer opportunities for engineering electronic and optical devices.[3–5] Many studies have centered on the control of morphology of rod–coil block copolymers. For instance, the two-component systems, such as AB rod–coil diblock copolymers and ABA rod–coil triblock copolymers, have been investigated both experimentally [6–9] and theoretically. [10–15] Many interesting microstructures, e.g., lamellae, arrowhead lamellae, zigzag lamellae, wave lamellae, strips, honeycombs, and hollow spherical and cylindrical micelles, have been found. The phase behavior of the two-component rod–coil block copolymers depends on three tunable parameters: the volume fraction of the rod block f_A, the Flory–Huggins interaction between different blocks χ_{AB}, and the total degree of polymerization of the copolymer N. As the species of the blocks of rod–coil block copolymers are increased from two to three, namely ABC triblock copolymer, the parameters governing the phase behavior become six: two independent volume fractions f_A and f_B, three different Flory–Huggins interactions between distinct species χ_{AB}, χ_{BC} and χ_{AC}, and the total degree of polymerization of the polymer chain N. This increased number of molecular variables will impose varieties and complexities on the self-assembly of the rod–coil block copolymer, meanwhile, leading to the possibilities of forming new self-assembled morphologies.

Experimentally, in comparison with rod–coil diblock copolymers, the self-assembly of ABC rod–coil triblock copolymers is less studied for its complexity. Lee and coworkers [8,16] studied ABC coil-rod–coil triblock and ABCBA coil-rod–coil-rod–coil pentablock molecules, which suggested a novel strategy to construct rich supramolecular nanostructures. Zhou et al. [17] reported an ABC coil-coil-rod triblock containing mesogen-jacketed liquid crystal polymer (MJLCP) as the rod block, and found the formation of a liquid crystalline phase when the rod block achieved a certain length. Despite these efforts, it remains challenging to understand well the mechanism of their self-assembly. With the development of computer science, simulation methods have been proved to be an effective approach to exploit the phase behavior of such complex systems. For example, by applying self-consistent field theory (SCFT) simulations, Tang et al. [18,19] and Tyler et al. [20,21] investigated the self-assembly of complex ABC flexible trilblock copolymers, where they successfully predicted interesting self-assembled structures that some of them were confirmed by subsequent experiments. [22–24] In the present report, we use the SCFT method to search for possible new morphologies formed in ABC rod–coil triblock copolymers, which is expected to provide guidance for the design and synthesis of such ABC materials.

* Corresponding authors. Tel.: +86 431 85262137; fax: +86 431 85262969.
** Corresponding author. Tel.: +86 431 85262206; fax: +86 431 85262126.
E-mail addresses: jzchen@ciac.jl.cn (J. Chen), ljan@ciac.jl.cn (L. An).

0032-3861/$ – see front matter © 2010 Elsevier Ltd. All rights reserved.
doi:10.1016/j.polymer.2010.04.063

The SCFT [25] has been exerted a powerful tool in predicting the morphologies of complex block copolymers, such as nonlinear shaped block copolymers, [19,26,27] multicomponent block copolymers [18–21,28], etc. Combined with other theoretical methods containing Flory's lattice theory, [29] Maier-Saupe theory [30] and Onsager theory [31] to account for the aligning interactions between rods, SCFT can also be used to study rod–coil block copolymer systems. Another group Li and Gersappe [32] studied the self-assembly of rod–coil diblock copolymers by proposing a lattice-based SCFT simulation where the aligning interactions between the rods can be ignored by employing the rotational isomeric state scheme. In this report, a SCFT lattice model is applied [12] and the rigid section of the copolymer is described similar to Li and Gersappe's method.

In earlier publications, we have used the SCFT lattice model to study the self-assembly of two-component rod–coil block copolymers. [12–14,33,34] We now extend it to the linear ABC coil-coil-rod triblock copolymers with three-components (as shown in Fig. 1) to explore the effect of broad parameter space on the self-assembly. We first concentrate on the copolymer with the coil blocks A and B having an equal length ($f_A = f_B$). To investigate the effects of the coil blocks A and B on the self-assembly, we then vary the relative length of the two coil blocks in term of keeping the length of the rod. Furthermore, by switching the sequence B and C, the effect of the block sequencing on the phase behavior is studied.

2. Theory

We consider a molten system of n linear ABC coil-coil-rod block copolymers and the total degree of polymerization of each chain is N, with compositions (average volume fraction) f_A and $f_B(f_C = 1 - f_A - f_B)$ respectively (Fig. 1). The segments of blocks A, B and C are supposed to have the same size and each segment occupies one lattice site, thus the total number of the lattice sites is $N_L = n(f_A N + f_B N + f_C N)$. For convenience, we use the segment size of block copolymer as the length unit. The transfer matrix lambda depends only on the used chain model. For a rod–coil system, we assume that

$$\lambda^{\alpha_{j,s}-\alpha'_{j,s-1}}_{r_{j,s}-r'_{j,s-1}} = \begin{cases} 1, & \alpha_{j,s} = \alpha'_{j,s-1} \\ 0, & \text{otherwise} \end{cases} \tag{1}$$

for the rod section and

$$\lambda^{\alpha_{j,s}-\alpha'_{j,s-1}}_{r_{j,s}-r'_{j,s-1}} = \begin{cases} 0, & \alpha_{j,s} = -\alpha'_{j,s-1} \\ 1/(z-1) & \text{otherwise} \end{cases} \tag{2}$$

for the coil section. Here, $r_{j,s}$ and $\alpha_{j,s}$ denote the position and bond orientation of the sth segment of the jth copolymer, respectively. The r' denotes the nearest neighboring site of r. We use the cubic lattice model which has six bond orientations and z is the coordination number of the lattice. Following the scheme of Scheutjens and Leermakers, [35] the end-segment distribution function $G^{\alpha_s}(r,s|1)$ that gives the statistical weight of all possible walks starting from segment 1, which may locate anywhere in the lattice, and ending at segment s at site r, is evaluated from the following recursive relation:

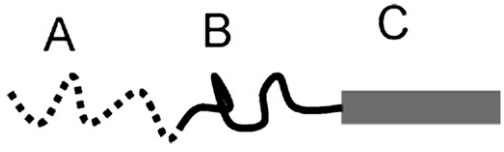

Fig. 1. Schematic illustration of the linear ABC coil-coil-rod triblock copolymer.

$$G^{\alpha_s}(r,s|1) = G(r,s)\sum_{r'_{s-1}}\sum_{\alpha'_{s-1}} \lambda^{\alpha_s-\alpha'_{s-1}}_{r_s-r'_{s-1}} G^{\alpha'_{s-1}}\left(r', s-1|1\right). \tag{3}$$

The initial condition is $G^{\alpha_1}(r,1|1) = G(r,1)$ for all values of α_1. The $G(r,s)$ is the free segment weighting factor and $G(r,s) = \begin{cases} \exp(-\omega_A(r_s)), & s\in A \\ \exp(-\omega_B(r_s)), & s\in B \end{cases}$. Another end-segment distribution function $G^{\alpha_s}(r,s|N)$ starting from the other chain end is evaluated from the following recursive relations:

$$G^{\alpha_s}(r,s|N) = G(r,s)\sum_{r'_{s+1}}\sum_{\alpha'_{s+1}} \lambda^{\alpha'_{s+1}-\alpha_s}_{r'_{s+1}-r_s} G^{\alpha'_{s+1}}\left(r', s+1|N\right) \tag{4}$$

with the initial conditions $G^{\alpha_N}(r,N|N) = G(r,N)$ for all the values of α_N.

The form of the free energy function of F (in the unit of k_BT) is analogous to our previous work [12]

$$\begin{aligned} F = &\frac{1}{z}\sum_{rr'}(\chi_{AB}\phi_A(r)\phi_B(r') + \chi_{AC}\phi_A(r)\phi_C(r') + \chi_{BC}\phi_B(r)\phi_C(r')) \\ &-\sum_r(\omega_A(r)\phi_A(r) + \omega_B(r)\phi_B(r) + \omega_C(r)\phi_C(r)) \\ &-\sum_r(\xi(r)(1-\phi_A(r)-\phi_B(r)-\phi_C(r))) - n\ln Q \end{aligned} \tag{5}$$

where

$$Q = \frac{1}{N_L}\frac{1}{z}\sum_{r_N}\sum_{\alpha_N} G^{\alpha_1}(r,1|N) \tag{6}$$

is the single-chain partition function. Here, χ_{AB}, χ_{AC}, χ_{BC} are Flory–Hugginns interaction parameters between different species. The $\phi_k(r)$ is the volume fraction field of block species k, which is independent of the individual polymer configuration, and $\omega_k(r)$ is the chemical potential field conjugated to $\phi_k(r)$. The $\xi(r)$ is the potential field that ensures the incompressibility of the system, also known as a Lagrange multiplier. Minimizing the free energy function F with respect to $\phi_A(r)$, $\phi_B(r)$, $\phi_C(r)$, $\omega_A(r)$, $\omega_B(r)$, $\omega_C(r)$ and $\xi(r)$ leads to the following SCFT equations:

$$\omega_A(r) = \frac{1}{z}\sum_{r'}\chi_{AB}\phi_B(r') + \frac{1}{z}\sum_{r'}\chi_{AC}\phi_C(r') + \xi(r), \tag{7}$$

$$\omega_B(r) = \frac{1}{z}\sum_{r'}\chi_{BC}\phi_C(r') + \frac{1}{z}\sum_{r'}\chi_{AB}\phi_A(r') + \xi(r), \tag{8}$$

$$\omega_C(r) = \frac{1}{z}\sum_{r'}\chi_{AC}\phi_A(r') + \frac{1}{z}\sum_{r'}\chi_{BC}\phi_B(r') + \xi(r), \tag{9}$$

$$\phi_A(r) + \phi_B(r) + \phi_C(r) = 1, \tag{10}$$

$$\phi_A(r) = \frac{1}{N_L}\frac{1}{z}\frac{n}{Q}\sum_{s\in A}\sum_{\alpha_s}\frac{G^{\alpha_s}(r,s|1)G^{\alpha_s}(r,s|N)}{G(r,s)}, \tag{11}$$

$$\phi_B(r) = \frac{1}{N_L}\frac{1}{z}\frac{n}{Q}\sum_{s\in B}\sum_{\alpha_s}\frac{G^{\alpha_s}(r,s|1)G^{\alpha_s}(r,s|N)}{G(r,s)}, \tag{12}$$

$$\phi_C(r) = \frac{1}{N_L}\frac{1}{z}\frac{n}{Q}\sum_{s\in C}\sum_{\alpha_s}\frac{G^{\alpha_s}(r,s|1)G^{\alpha_s}(r,s|N)}{G(r,s)}. \tag{13}$$

In our calculations, the real-space method is implemented to solve the SCF equations in a cubic lattice with periodic boundary conditions, which is similar to our previous reports. [12–14] To prevent bias of the resulting morphologies, our calculations are initiated with different random-generated fields. The calculation

stops when the free energy changes within a tolerance of 10^{-8}. The obtained morphologies correspond to either a stable or a metastable state. By comparing the free energy of the system, the relative stability of the morphologies can be assessed.

3. Results and discussion

In our studies, the interactions between the species are set to be the same, i.e., $\chi = \chi_{AB} = \chi_{BC} = \chi_{AC}$, and the total degree of polymerization of the linear ABC coil–coil–rod triblock copolymers is $N = 20$. Thus, the ordered morphologies of the copolymers depend on three tunable molecular parameters: f_A(the volume fraction of the coil block A), f_C (the volume fraction of the rod block C), χ(the Flory–Huggins interaction between different species). Fig. 2 shows all the morphologies discovered in this study, where three different colors, blue, green, and red are, respectively, assigned to A, B and C blocks, and some components are eliminated for the sake of a clear presentation. For the linear ABC coil-coil-rod triblock copolymer, we first focus on the copolymer with an equal length of A and B coil blocks i.e., $f_A = f_B$, and the phase diagram constructed by f_{rod} versus χN is present in Fig. 3. To investigate the effects of the A and B coil blocks on the self-assembly of the copolymers, we then tune the relative length of the two coil blocks while keeping the length of the rod, and the phase diagrams constructed by f_A versus χN are shown in Fig. 4. Furthermore, by switching the sequence of the block A-B-C to A-C-B, a linear ACB coil-rod–coil triblock copolymer is obtained, by which the effect of the block sequencing on the phase behavior is presented. The calculations are preformed in $N_L = 60^3$ to $N_L = 80^3$ lattices to make sure that the emergence of the self-assembled structures are not constrained by system size and

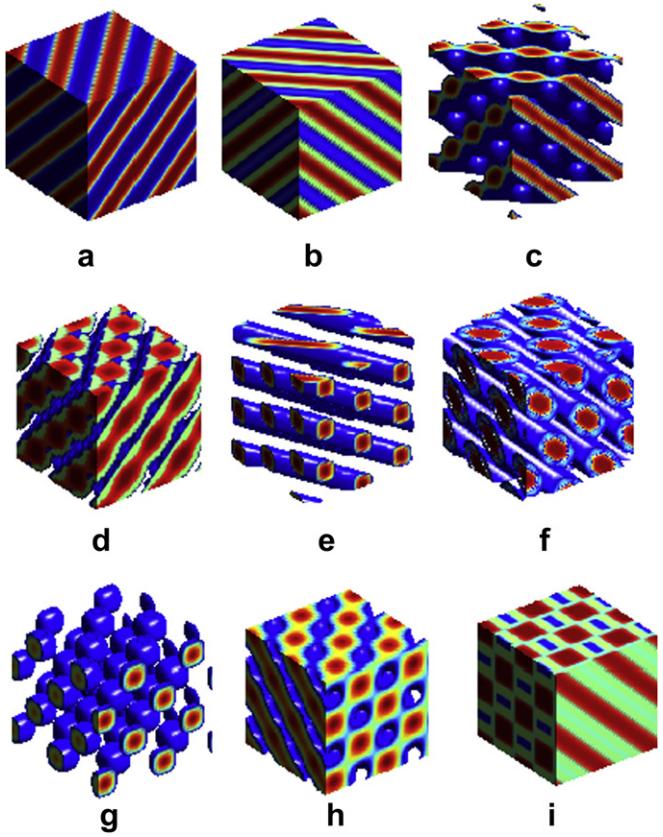

Fig. 2. Ordered morphologies obtained in our present work. (a) "two-color" lamellar phase (LAM2); (b) "three-color" lamellar phase (LAM3); (c) "two-color" perforated lamellar phase (PL2, the components A and B are eliminated for clarity); (d) "three-color" perforated lamellar phase (PL3, the component A is eliminated for clarity); (e) strip (S, the components A and B are eliminated for clarity); (f) core-shell hexagonal lattice phase (CSH, the component A is eliminated for clarity); (g) micelle (M, the components A and B are eliminated for clarity); (h) gyroid (G, the components A and B are eliminated for clarity); (i) metastable interpenetrated hexagonal lattice phase (HEX2).

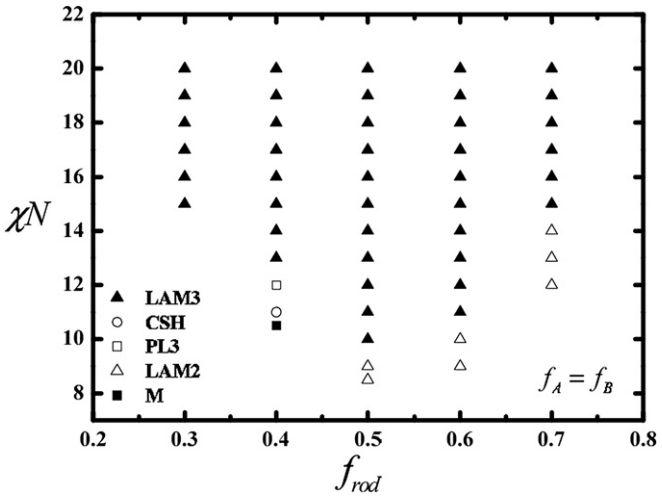

Fig. 3. Phase diagram is shown for the linear ABC coil–coil–rod triblock copolymer ($f_A = f_B$).

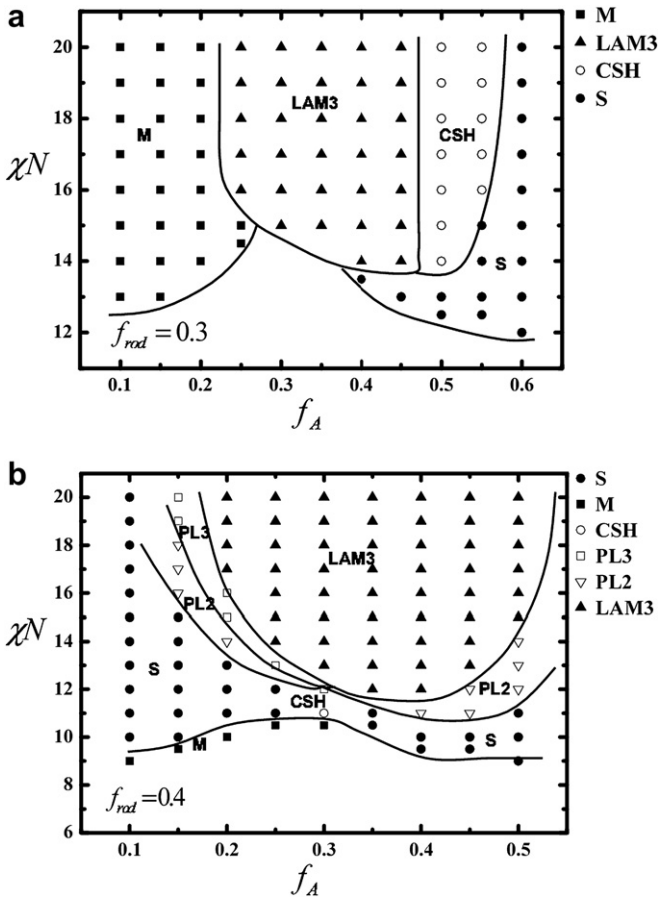

Fig. 4. Phase diagrams are shown for the linear ABC coil–coil–rod triblock copolymer for (a) $f_{rod} = 0.3$ and (b) $f_{rod} = 0.4$. The solid lines are not exact boundaries but are visual guides separating the regions of the morphologies.

the simulations start from both ordered and random configurations to ensure that the observed structure are not kinetically arrested but equilibrium structures. Below we proceed with a detailed discussion of the simulation results.

When the A and B coil blocks are equal ($f_A = f_B$), five stable morphologies are formed, i.e., "two-color" lamella (LAM2), "three-color" lamella (LAM3), "three-color"-perforated lamella (PL3), core-shell hexagonal lattice phase (CSH) and micelle (M) as shown in Fig. 2, and the distribution of these structures in the phase diagram is presented in Fig. 3. Noticeably, the lamellae are found stable in the most regions in the phase diagram. By implementing further calculations, [12] the rods of the linear ABC coil-coil-rod triblock copolymers in the lamellae are found to orient in a common direction. Considering the competition between the rods attempting to maximize their contact with other rods to minimize energy and the coil blocks attempting to maximize their free volume to maximize entropy, the former plays a major role when the rod volume fraction is high, i.e., $f_{rod} \geq 0.5$, and results in the formation of the lamellar structure for the linear ABC coil-coil-rod triblock copolymers. As the rod volume fraction is lowered, i.e., $f_{rod} < 0.5$, the coil blocks tend to maximize their free volume to maximize entropy, and the nonlamellar structures are found for rod–coil diblock copolymers. [11,12,36] However, for the linear ABC coil-coil-rod triblock copolymers, due to the incompatibility between the A and B coil blocks, the lamellar structure still remains stable. The LAM2 is stable under the LAM3 in the phase diagram for the reason that the A and B coil blocks do not microsegregate in those degree of segregation and diffuse together to form an alternate layer of the lamella. Besides, for the linear ABC coil-coil-rod triblock copolymers, rich order–order phase transitions are expected to happen when $f_{rod} = 0.4$, i.e., the ordered morphologies change from M, to CSH, to PL3, and finally to LAM3 with decreasing temperature, indicating that the self-assembly of linear ABC coil-coil-rod is subtle to the temperature.

To investigate the effects of the A and B coil blocks on the self-assembly of the linear ABC coil-coil-rod triblock copolymers, we vary the relative length of the two coil blocks while keeping the length of the rod. When $f_{rod} \geq 0.5$, the lamellae are formed regardless of the relative length of the A and B coil blocks (the phase diagrams are not shown), for the reason that the effects of the rods attempting to maximize their contact with other rods to minimize energy is dominant as discussed above. When $f_{rod} < 0.5$, the effect of the coil blocks tend to compete for that of rod blocks, leading to various phase behaviors by varying the relative length of the A and B coil blocks for the linear ABC coil-coil-rod triblock copolymer. The phase diagrams are constructed with f_A versus χN with fixed rod volume fractions $f_{rod} = 0.3$ and 0.4 respectively. As shown in Fig. 4 (a–b), the lamellar structure is found stable near the region where the A and B coil blocks have an equal length, i.e., $f_A = f_B = 0.35$ for $f_{rod} = 0.3$ and $f_A = f_B = 0.3$ for $f_{rod} = 0.4$. When the relative length of the A and B coil blocks becomes asymmetric, i.e., further increasing the coil block A while decreasing the coil block B or decreasing the coil block A while increasing the coil block B, the nonlamellar structures appears, where the system tends to make more room for the coil blocks to maximize entropy. When $f_A < f_B$, with the decreasing volume fraction of coil block A, the self-assembly of the linear ABC coil-coil-rod triblock copolymers quickly reduces to that of coil-rod diblock copolymers, such as the fact that the ordered morphologies change from LAM3 to M for $f_{rod} = 0.3$ and $f_A < 0.25$, and from LAM3 to PL3, to PL2 and finally to S for $f_{rod} = 0.4$ and $f_A < 0.15$. When $f_A > f_B$, with the increasing volume fraction of the coil block A, the morphologies of the linear ABC coil-coil-rod triblock copolymers change from LAM3, to CSH, and finally to S for $f_{rod} = 0.3$, and from LAM3 to PL2for $f_{rod} = 0.4$, which shows that the phase behavior of the triblock copolymer also tends to turn to that of coil-rod diblock copolymers but cannot be expected to be exactly the same even if the volume fraction of the coil block B is small ($f_B = 0.1$). Besides, an interesting metastable phase, namely interpenetrating hexagonal lattice (HEX2), is formed in a very limited region $f_A = 0.2$ and $\chi N > 15$, where the component A and C (rod) form the strips respectively with the component B forming the continuous matrix as shown in Fig. 2. The similar interpenetrating microstructure has been reported in the self-assembly of linear ABC coil–coil–coil triblock copolymers in Tang's work, [18] where, however, the interpenetrating microstructure is a stable one. Compared with the linear ABC coil-coil-coil triblock copolymer, the self-assembly of the linear ABC coil-coil-rod triblock copolymer introduce the interaction of the rods which plays a crucial role in the phase behavior. Our calculation also proves that the rods of the linear ABC coil-coil-rod triblock copolymer in the HEX2 phase prefer to orient in a common direction rather than pack in an interdigited fashion like that of coil-rod diblock copolymers, [12] which makes the free energy of HEX2 higher than that of LAM3 structure.

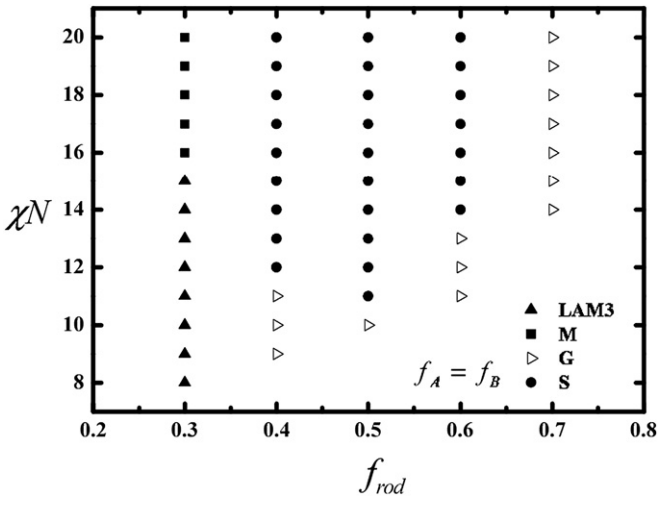

Fig. 5. Phase diagram is shown for the linear ACB coil–rod–coil triblock copolymer ($f_A = f_B$).

By switching the sequence of the blocks B and C in the polymer chain, an ACB coil–rod–coil triblock copolymer is obtained and we focus on the copolymer with the A and B coil block having an equal length. Four morphologies, i.e., LAM3, M, G and S (as shown in Fig. 2), are found stable, and the distribution of these structures is presented in Fig. 5. Different from the ABC coil–coil–rod triblock copolymers, the gyroid and the strip structures are found sable at relatively high rod volume fractions, i.e., $f_{rod} \geq 0.4$, which can be attributed to the fact that both ends of the rods are strongly constrained by the A and B coil blocks for the ACB coil–rod–coil triblock copolymer.

4. Conclusions

As an extension of our previous works, the self-assembly of the linear ABC coil-coil-rod triblock copolymers was investigated based on real-space SCF-lattice techniques in three-dimensional space. Compared with rod–coil diblock copolymers, our results revealed the effects of the broad parameter space on the self-assembly of the linear ABC coil-coil-rod triblock copolymers. Seven stable morphologies were observed, including "two-color" lamella, "three-color" lamella, "two-color"-perforated lamella, "three-color"-perforated lamella, core-shell hexagonal lattice phase, strip, and micelle. When the length of the A and B coil blocks is equal ($f_A = f_B$), the lamellae were found to be stable in the most regions of the phase diagram, which could be attributed to the incompatibility

between the two coil blocks. When $f_A < f_B$, the self-assembly of the linear ABC coil-coil-rod triblock copolymer quickly reduced to that of coil-rod diblock copolymer for $f_{rod} = 0.3$, $f_A < 0.25$ and $f_{rod} = 0.4$, $f_A < 0.15$ with deceasing volume fraction of coil block A. When $f_A > f_B$, the phase behavior of the triblock copolymer also tends to turn to that of coil-rod diblock copolymer but cannot be expected to be exactly the same even if the volume fraction of the coil block B is decreased to a small one ($f_B = 0.1$). By calculating the self-assembly of linear ACB coil-rod–coil triblock copolymers, the block sequencing is described to impose profound effects on the self-assembly of the copolymer. These simulation results we present are expected to provide guidance to design the desired microphases in the complex rod–coil block copolymers. The results presented above are based on the assumption that the Flory–Huggins interaction parameters are symmetric, where we mainly concentrate on the effect of the rod block of the ABC coil-rod triblock copolymer on the self-assembly behavior. We also note that the asymmetric Flory–Huggins parameters play an important role in the self-assembly of the ABC triblock copolymers, as reported by Tang et al. [18] and Tyler et al. [21] for the ABC coil-coil-coil triblock copolymer. In our ABC rod–coil systems, the asymmetric interaction parameters can also be turned, by which the packing style of the rods may be manipulated and interesting morphologies are expected to form in the self-assembly. This investigation will be implemented in a subsequent work.

Acknowledgments

This work is supported by the National Natural Science Foundation of China (20804047, 20774096, 20734003) Programs and the Fund for Creative Research Groups (50921062), and subsidized by the Special Funds for National Basic Research Program of China (2009CB930100, 2010CB631100).

References

[1] Lecommandoux S, Achard MF, Langenwalter JF, Klok HA. Macromolecules 2001;34:9100.
[2] Losik M, Kubowicz S, Smarsly B, Schlaad H. Eur Phys J E 2004;15:407.
[3] Ball ZT, Sivula K, Frechet JMJ. Macromolecules 2006;39:70.
[4] Van De Wetering K, Brochon C, Ngov C, Hadziioannou G. Macromolecules 2006;39:4289.
[5] Dai CA, Yen WC, Lee YH, Ho CC, Su WF. J Am Chem Soc 2007;129:11036.
[6] Lee M, Cho BK, Zin WC. Chem Rev 2001;101:3869.
[7] Chen JT, Thomas EL, Ober CK, Hwang SS. Science 1997;273:343.
[8] Oh NK, Zin WC, Im JH, Lee M. Polymer 2006;47:5275.
[9] Lin J, Zhu G, Zhu X, Lin S, Nose T, Ding W. Polymer 2008;49:1132.
[10] Muller M, Schick M. Macromolecules 1996;29:8900.
[11] Horsch MA, Zhang Z, Glotzer SC. Phys Rev Lett 2005;95:056105.
[12] Chen JZ, Zhang CX, Sun ZY, Zheng YS, An LJ. J Chem Phys 2006;124:104907.
[13] Chen JZ, Zhang CX, Sun ZY, An LJ, Tong Z. J Chem Phys 2007;127:024105.
[14] Chen JZ, Sun ZY, Zhang CX, An LJ, Tong Z. J Chem Phys 2008;128:074904.
[15] He L, Zhang L, Liang H. Polymer 2009;50:721.
[16] Lee M, Lee DW, Cho BK. J Am Chem Soc 1998;120:13258.
[17] Zhang H, Sun X, Wang X, Zhou Q. Macromol Rapid Commun 2005;26:407.
[18] Tang P, Qiu F, Zhang H, Yang Y. Phys Rev E 2004;69:031803.
[19] Tang P, Qiu F, Zhang H, Yang Y. J Phys Chem B 2004;108:8434.
[20] Tyler CA, Morse DC. Phys Rev Lett 2005;94:208302.
[21] Tyler CA, Qin J, Bates FS, Morse DC. Macromolecules 2007;40:4654.
[22] Chatterjee J, Jain S, Bates FS. Macromolecules 2007;40:2882.
[23] Takano A, Wada S, Sato S, Araki T, Hirahara K, Kazama T, et al. Macromolecules 2004;37:9941.
[24] Tureau MS, Epps TH. Macromol Rapid Commun 2009;30:1751.
[25] Matsen MW, Schick M. Phys Rev Lett 1994;72:2660.
[26] Wang R, Xu T. Polymer 2007;48:4601.
[27] Ye X, Shi T, Lu Z, Zhang C, Sun Z, An L. Macromolecules 2005;38:8853.
[28] Jiang Y, Yan X, Liang H, Shi A. J. Phys Chem B 2005;109:21047.
[29] Matsen MW, Barrett C. J Chem Phys 1998;109:4108.
[30] Pryamitsyn V, Ganesan V. J Chem Phys 2004;120:5824.
[31] Song W, Tang P, Zhang H, Yang Y, Shi A. Macromolecules 2009;42:6300.
[32] Li WT, Gersappe D. Macromolecules 2001;34:6783.
[33] Xia Y, Sun Z, Shi T, Chen J, An L, Jia Y. Polymer 2008;49:5596.
[34] Xia Y, Chen J, Sun Z, Shi T, An L, Jia Y. J Chem Phys 2009;131:144905.
[35] Leermakers FAM, Scheutjens JMHM. J Chem Phys 1988;89:3264.
[36] Reenders M, Brinke Gt. Macromolecules 2002;35:3266.